

Journal of Materials Chemistry A

Accepted Manuscript



This is an *Accepted Manuscript*, which has been through the Royal Society of Chemistry peer review process and has been accepted for publication.

Accepted Manuscripts are published online shortly after acceptance, before technical editing, formatting and proof reading. Using this free service, authors can make their results available to the community, in citable form, before we publish the edited article. We will replace this *Accepted Manuscript* with the edited and formatted *Advance Article* as soon as it is available.

You can find more information about *Accepted Manuscripts* in the [Information for Authors](#).

Please note that technical editing may introduce minor changes to the text and/or graphics, which may alter content. The journal's standard [Terms & Conditions](#) and the [Ethical guidelines](#) still apply. In no event shall the Royal Society of Chemistry be held responsible for any errors or omissions in this *Accepted Manuscript* or any consequences arising from the use of any information it contains.

Cite this: DOI: 10.1039/c0xx00000x

www.rsc.org/xxxxxx

ARTICLE TYPE

A Magnesium Tetraphenylaluminate Battery Electrolyte Exhibits a Wide Electrochemical Potential Window and Reduces Stainless Steel Corrosion

Emily G. Nelson,^a Scott I. Brody,^a Jeff W. Kampf^a and Bart M. Bartlett^{*a}

⁵ Received (in XXX, XXX) Xth XXXXXXXXX 20XX, Accepted Xth XXXXXXXXX 20XX
DOI: 10.1039/b000000x

Using Al(OPh)₃ rather than the typical AlCl₃ with Grignard reagents affords a Mg-ion electrolyte with a reduced chloride content. A 1:4 Al(OPh)₃:PhMgCl mixture gives a magnesium tetraphenylaluminate salt that exhibits anodic stability up to 5 V vs Mg^{2+/0} on both platinum and stainless steel working electrodes and, shows much reduced corrosion (pitting) of stainless steel after extended electrolysis at 4.5 V.

With the increased interest in sustainable energy has come a substantial investment in advanced energy storage systems.¹ Of the storage systems investigated, lithium-ion batteries have seen the greatest commercial success with incorporation into hybrid electric vehicles. However, they are still not able to meet the energy density requirements for all-electric vehicles to become competitive in driving range and cost compared to traditional internal combustion engine vehicles. There are also safety concerns due to the low overpotential associated with Li⁺ reduction to metallic dendrites that lead to short-circuit pathways. An alternative which has received much attention is the magnesium-ion battery.^{2,3} Mg-ion research is still in the basic stages of development, but Mg is promising due to its fairly negative potential and larger volumetric capacity with its two-electron couple. Magnesium is also considered safer owing its tendency to deposit in dense, cube-like structures rather than dendrites.⁴⁻⁶

Progress in Mg-based batteries systems has been hampered for several reasons. First, most electrolytes are composed of air- and moisture sensitive Grignard reagents, and they are limited to flammable and volatile ethereal solvents such as THF. These drawbacks increase the safety concerns with producing magnesium batteries on commercial scale. Compared to electrolytes used in lithium-ion batteries, magnesium-based electrolytes at present show much narrower potential windows. There is a recent example in pushing the anodic stability to nearly 4 V (vs. Mg^{2+/0}), but this electrolyte relies on boron/Lewis-base adducts.⁷ Second, the paucity of electrolytes exhibiting large stability windows impedes the development of novel high-voltage cathode materials.⁸ Finally, although the electrochemical window of an electrolyte in a particular solvent is dictated by the HOMO of the most oxidizable species and LUMO of the most reducible species, many combinations that are electrochemically inert using platinum as the working electrodes fail to show the same stability

50
55

on common non-noble metal current collectors such as stainless steel.^{7,9} This decrease in the usable potential window is attributed to corrosion reactions occurring on the electrode, and is thought to arise due to the high chloride content of these common electrolytes.¹⁰ One way to circumvent this shortcoming is to develop new current collectors that are compatible with current magnesium-ion electrolytes.^{11,12} However, this approach will require complete re-engineering of current battery systems that are based largely on stainless steel. Instead, we have focused on altering the electrolyte composition to decrease the chloride content.

Our group and others have previously shown that replacing the phenyl group (R = Ph) in RMgCl with phenolate (R = OPh) gives rise to greater air and moisture stability of the Lewis bases commonly used as precursors in electrolyte solutions.^{13,14} The other precursor is the Lewis acid AlCl₃. Structural characterization of the electrolyte solutions shows ligand exchange to generate a [Mg₂Cl₃]⁺ and [Al(OR)₄]⁻ ion pair in solution. Although these electrolytes perform well, they still contain a relatively high chloride content, and corrosion of non-noble metal current collectors remains problematic.

To reduce the chloride content, we have prepared an electrolyte starting from the Lewis acid Al(OPh)₃. Al(OPh)₃ was synthesized by reacting three equivalents of phenol with Me₃Al

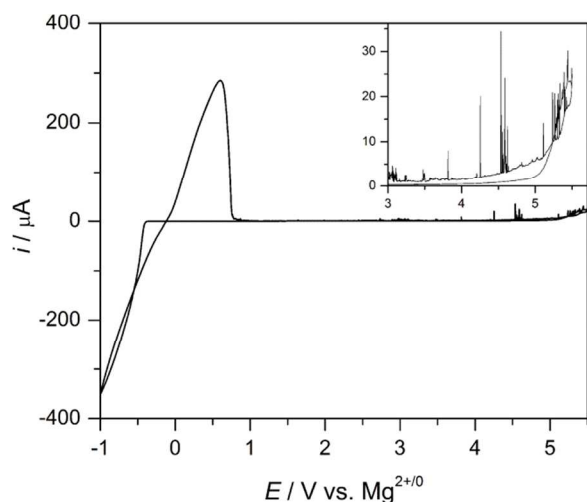


Figure 1. CV of a solution of 0.5 M Al(OPh)₃/PhMgCl in THF on a Pt working electrode at a scan rate of 25 mV/s. Inset shows close up of oxidation potential.

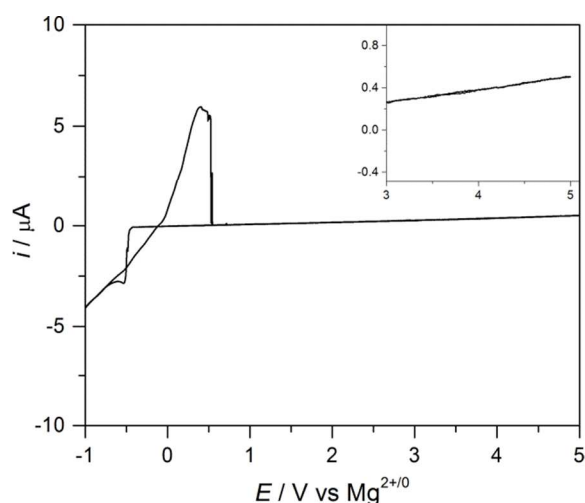


Figure 2. Cyclic voltammogram of an electrolyte solution of 0.5 M Al(OPh)₃/PhMgCl in THF recorded on a 316 stainless steel micro-working electrode at a scan rate of 25 mV/s.

under inert atmosphere. This product reacts with the Grignard reagent PhMgCl in THF (also carried out under inert atmosphere) to form the electrolyte (1 Al(OPh)₃ : 4 PhMgCl, with complete experimental details available in the ESI.) The conductivity of the electrolyte at 0.5 M (based on total Mg²⁺ concentration), is 1.24 mS/cm, which is within the reported range of common Mg-ion electrolytes.^{15–17}

The cyclic voltammogram (CV) in Figure 1 shows anodic stability out to 5 V vs. Mg^{2+/0} on Pt. Although we sacrifice air- and moisture stability, we have generated an electrolyte that allows us to work approximately 1 V more positive than that of the best previously reported electrolyte.⁷ The inset clearly shows random, positive current spikes on the anodic side. Similar observed behavior as well as the limited anodic stability limit of THF solvent (only 3.5 V) suggests the possible formation of a quasi-passivation layer on Pt.¹⁸ This behavior appears to be unique to the presence of tetraphenyl-aluminate, and it is hypothesized the phenyl groups create a specific adsorption of Al(Ph)₄⁻ molecules on the Pt surface, resulting in a break-and-repair-like mechanism. In an effort to examine this possibility,

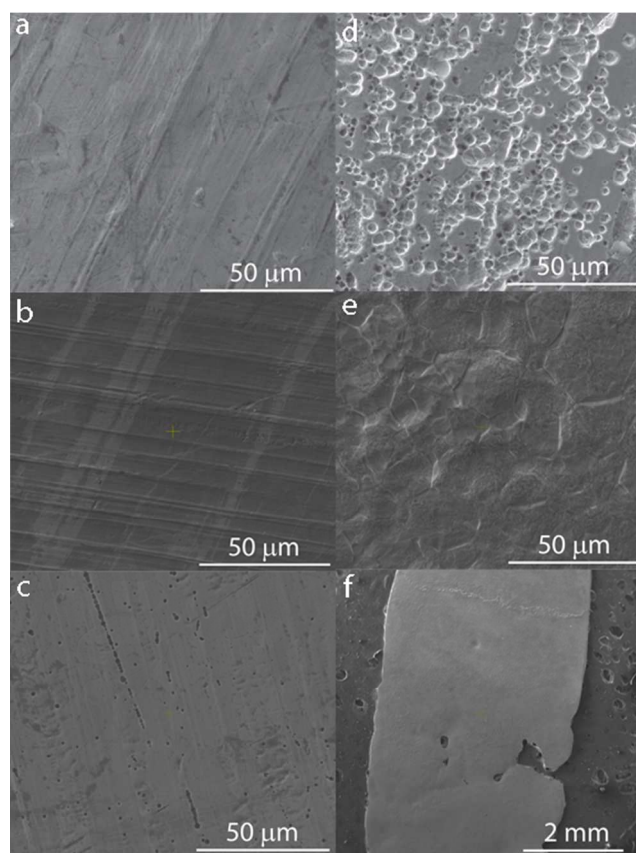


Figure 3. SEM images of stainless steel a) before exposure to Mg electrolyte; b) after one CV cycle from 0 – 5.0 V in Al(OPh)₃/PhMgCl; c) after electrolysis at 4.5 V for 96 hours in Al(OPh)₃/PhMgCl; d) after one CV cycle from 0 – 4.0 V in APC; e) after electrolysis at 4.0 V for 24 hours in APC; f) after electrolysis at 4.0 V for 24 hours in APC.

XP spectra of the Pt foil before and after cycling in the electrolyte solution are presented as Figures S1 – S3 in the ESI. Fitting the C(1s) peak after cycling in the electrolyte shows a new peak at 290.5 eV. This broad peak is ascribed to $\pi - \pi^*$ shake up peak, attributed to benzene/phenyl carbon. The complete absence of an Al(2s) peak after cycling demonstrates that the 290.5 eV peak does not result from adsorbed AlPh₄⁻, but hints at the possibility of free benzene/phenyl carbon adsorbed to Pt after electrochemical cycling. We note, however that although the presence of this peak after cycling suggests a surface interaction between the electrolyte, it does not necessarily prove that it is electrochemically passivating. Adding benzene and phenol to a solution of APC does not improve the electrochemical stability on Pt which lends further support to the absence of a ligand-based electrochemical passivation layer (Figure S4). Combined AFM-SECM measurements that are beyond the scope of this work are planned to probe this electrode/electrolyte interface further.

Magnesium deposition was confirmed by analyzing copper foil electrode following galvanostatic deposition (2 mA/cm², 2.3 C/cm²). The SEM image and EDX analysis show only Mg⁰ deposition in a dense, dendrite free morphology (Figure S5). The deposition and stripping events show low overpotentials of 0.47 and 0 V respectively and excellent coulombic efficiency (~98%, Figure S6).

Since chloride is implicated in corrosion on stainless steel, and our 1:4 Al(OPh)₃-PhMgCl electrolyte system contains a lower chloride concentration, we expect to see greater stability on stainless steel. Indeed, a CV of our Al(OPh)₃-PhMgCl electrolyte on stainless steel in Figure 2 shows that anodic stability is maintained out to ~5 V vs Mg^{2+/0}, much more positive than any previously reported electrochemical performance on stainless steel. It is interesting to note the absence of positive spikes in current in the CV on stainless steel. We hypothesize the Al(Ph)₄⁻ and/or benzene/phenyl species do not exhibit adsorption onto stainless steel, and thus a break-and-repair-like mechanism is not observed. This hypothesis is supported by the absence of additional carbon species on the stainless steel foil after cycling in the electrolyte by XPS (Figure S7).

To examine the increased performance on stainless steel further, a series of SEM images of the stainless steel foil are presented in Figure 3. Figure 3a shows the stainless steel prior to being exposed to electrolyte. After electrolysis in our Al(OPh)₃/PhMgCl electrolyte (by cyclic voltammetry, Figure 3b or under controlled potential coulometry, Figure 3c) the morphology of the stainless steel is virtually unchanged. For comparison, we synthesized the known AlCl₃/PhMgCl (APC) electrolyte.¹⁷ After a single CV sweep in the APC electrolyte, the stainless steel shows a high density of pitting (Figure 3d) that only gets worse under bulk electrolysis (Figures 3e and f). The anodic stability limit for THF is estimated to be ~3.5 V vs. Mg^{2+/0}, far below the stability shown here on both Pt and SS electrodes.

To ensure that this enhanced stability is due to the electrolyte, and not simply the formation of a passivation layer, we carried out intercalation studies. In the absence of a high-voltage magnesium cathode, reversible insertion/extraction was performed with the spinel lithium cathode LiMn₂O₄. A 2016-type coin cell composed of 0.5 M Al(OPh)₃/PhMgCl in THF containing 0.5 M LiPF₆, a LiMn₂O₄ cathode, and a Mg foil anode was charged and discharged at room temperature at C/5 current (105 μA/cm²). Details of cell assembly are included in the ESI. A CV of the electrolyte with LiPF₆ was performed to ensure that adding the lithium salt does not interfere with electrolyte performance (Figure S8). Figure 4 shows the charge-discharge

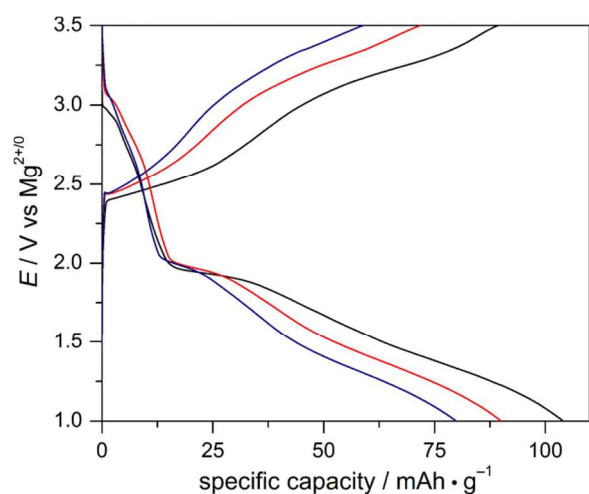


Figure 4. Typical charge/discharge profiles for a rechargeable battery with a LiMn₂O₄ cathode, 0.5 M Al(OPh)₃/PhMgCl in THF with 0.5 M LiPF₆, a Mg anode at cycles 1 (black), 5 (red), and 20 (blue).

curves within the voltage window 1.0 – 3.5 V vs Mg^{2+/0}. We note that the discharge capacities are larger than the charge capacities with an initial discharge capacity of ~100 mAh/g, and initial charge capacity of ~90 mAh/g. This is likely due to some insertion of Mg²⁺ into the Li⁺ channels of the spinel structure upon discharge, resulting in the increased discharge capacity. The insertion of Mg²⁺ into the cathode is also likely the cause of the rapid capacity fade, as the insertion of magnesium in the smaller lithium channels of the spinel is expected to be irreversible. Despite the presence of this fade, the LiMn₂O₄ cathode does show the ability to insert/extract Li⁺ in the presence of the magnesium-based electrolyte. This result suggests that Al(OPh)₃/PhMgCl does not undergo electrochemical degradation within this potential range, testifying to the stability of this electrolyte to 3.5 V vs. Mg^{2+/0}. To ascertain the stability of stainless steel with our electrolyte further, we examined the coin cell casing after cycling the LiMn₂O₄ cathode. The images presented in Figure S9 show no pitting after cycling 100 times to 3.5 V.

Although Li⁺ insertion/extraction demonstrates electrolyte stability, we must also show reversible Mg²⁺ insertion/extraction into a true magnesium host material. Accordingly, we tested the compatibility of Al(OPh)₃/PhMgCl with a WSe₂ cathode, which has been shown to intercalate Mg²⁺ reversibly.¹⁹ WSe₂ is isostructural with MoO₂, and was synthesized by a solid state route.²⁰ Plate-like particles range from 2 – 10 μm in size (Figure S10). A 2016-type coin cell comprised of 0.5 M Al(OPh)₃/PhMgCl in THF, the WSe₂ cathode, and Mg foil anode was charged and discharged at room temperature at C/5 (12 μA/cm²) current. Figure 5 shows the voltage-capacity profiles for the 5th, 10th, 20th, and 50th galvanostatic cycles. The discharge capacity is ~80 mAh/g, consistent with reversible Mg²⁺ insertion into WSe₂. The polarization between the charge and discharge curves is likely due to the large particle size of the WSe₂ that results from the solid state synthesis, and we note that the polarization does not increase with continued cycling. The use of a 2.5 V cathode does not begin to approach the apparent upper limit of the electrolyte stability, and recent work has resulted in developing higher voltage cathodes, which we have begun to explore.^{21,22} Although the Mo₆S₈ Chevrel-phase cathode exhibits

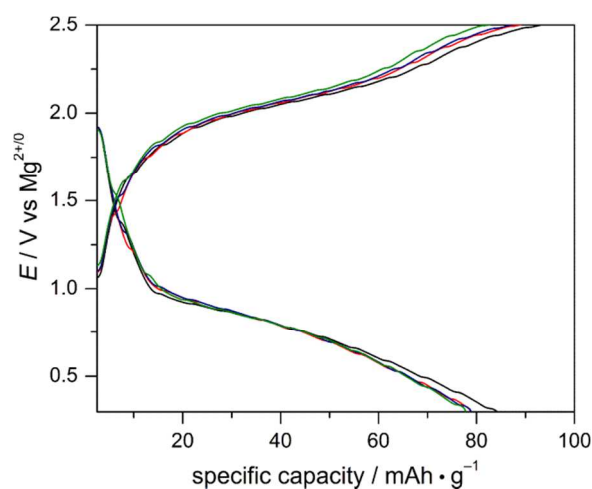


Figure 5. Typical charge/discharge profiles for a rechargeable battery with Al(OPh)₃/PhMgCl in THF, a Mg anode, a WSe₂ cathode at cycles 5 (black), 10 (red), 20 (blue), and 50 (green).

a lower cut off voltage of 1.2 V vs $\text{Mg}^{2+/0}$, we have also cycled $\text{Al}(\text{OPh})_3/\text{PhMgCl}$ with the Mo_6S_8 cathode materials (Figure S11).

Initial structural characterization by multinuclear NMR spectroscopy and ESI-MS⁻ analysis of our electrolyte solution show that the $[\text{AlPh}_4]^-$ anion is the dominant species in solution, and it results from ligand exchange between the aluminum and magnesium starting materials (Figures S12–S13). Previous DFT calculations suggest that AlPh_4^- is more susceptible to oxidation than AlCl_4^- , although this result is not experimentally observed.²³ $[\text{Al}(\text{Ph})_3(\text{OPh})]^-$ as well as a few other aluminum complexes make up smaller contributions to the solution speciation. Switching to ESI-MS⁺ mode shows the presence of the most common chloro-bridged $[\text{Mg}_2\text{Cl}_3(\text{THF})_4]^+$ dimer as well as the phenolate-bridged species $[\text{Mg}_2(\text{OPh})_3\text{Cl}(\text{THF})_2]^+$ (Figure S14). Two different neutral magnesium phenolate complexes have been crystallized successfully from the 1:4 $\text{Al}(\text{OPh})_3$: PhMgCl electrolyte mixture, and their X-ray crystal structures are presented in Figure S15–S16. The $[\text{Mg}_2\text{Cl}_3]^+$ cation is most commonly named as the “active” Mg^{2+} species in solution, although recent work suggests it may in fact only be a precursor to the ionically conductive species from which Mg^0 deposits.²⁴ Because we observe two distinct Mg^{2+} species in solution, it is unclear as to which one contributes to Mg^0 deposition (or if both do), and elucidating this result is beyond the scope of this initial report. However, we are presently developing synthesis methods for preparing these species independently to measure the corresponding rates of Mg^0 deposition from each.

Conclusions

Eliciting the factors relevant for controlling oxidative stability and improving the compatibility of Mg-ion electrolytes with commercially relevant current collectors and battery casings such as stainless steel is crucial for the next-generation (beyond Li-ion) electrical energy storage. Here, we have shown that decreasing the chloride content in Mg-ion electrolytes by switching the Lewis acid from AlCl_3 to $\text{Al}(\text{OPh})_3$ greatly improves the stability on both Pt and stainless steel electrodes. We observe minimal pitting on stainless steel after electrolysis at 4.5 V vs $\text{Mg}^{2+/0}$ for 96 hours compared to the extreme pitting observed in the more widely reported APC electrolyte after only 24 hours. Through cycling with LiMn_2O_4 , we have verified the stability of this electrolyte up to 3.5 V, and studies to probe its full electrochemical window are underway. The unprecedented stability of this electrolyte suggests that the stability may be explained by more than simply eliminating chloride from the starting Lewis acid. In particular, an in depth examination of solution speciation is underway in an effort to determine what molecular species result in reversible deposition/stripping electrochemical performance.

Acknowledgements

This research was supported by a grant from the National Science Foundation (DMR-1253347). SEM imaging and XPS was carried out with the assistance of James J. Brancho and Kayla Pyper at the University of Michigan Electron Microbeam Analysis Laboratory, and was funded by the NSF (DMR-0320740). We

thank Dr. Joseph E. Yourey for assistance preparing the WSe_2 active electrode material.

Notes and references

- ⁶⁰ ^a Department of Chemistry, University of Michigan, 930 N. University Avenue Ann Arbor 48109-1055, USA. Fax: (+) 1-734-647-4865; E-mail: bartmb@umich.edu
- † Electronic Supplementary Information (ESI) available: [details of any supplementary information available should be included here]. See DOI: 10.1039/b000000x
- Z. G. Yang, J. L. Zhang, M. C. W. Kintner-Meyer, X. C. Lu, D. W. Choi, J. P. Lemmon, J. Liu, *Chem. Rev.*, 2011, **11**, 3577.
 - T. D. Gregory, R. J. Hoffman, R. C. Winterton, *J. Electrochem. Soc.*, 1990, **137**, 775.
 - D. Aurbach, Z. Lu, A. Schechter, Y. Gofer, H. Gizbar, R. Turgeman, Y. Cohen, M. Moshkovich, E. Levi, *Nature*, 2000, **407**, 724.
 - C. Ling, D. Banerjee, M. Matsui, *Electrochim. Acta*, 2012, **76**, 270.
 - D. Aurbach, A. Schechter, M. Moshkovich, Y. Cohen, *J. Electrochem. Soc.*, 2001, **148**, A1004.
 - D. Aurbach, I. Weissman, Y. Gofer, E. Levi, *Chem. Record*, 2003, **3**, 61; Z. Feng, Y. NuLi, J. Wang, J. Yang, *J. Electrochem. Soc.*, 2006, **153**, C689; L. Gaddum, H. French, *J. Am. Chem. Soc.*, 1927, **49**, 1295.
 - Y. Guo, F. Zhang, J. Yang, F. Want, Y. NuLi, S. Hirano, *Energy Environ. Sci.*, 2012, **5**, 9100.
 - T. Ichitsubo, T. Adachi, S. Yagi, T. Doi, *J. Mater. Chem.*, 2011, **21**, 11764.
 - J. Muldoon, C. Bucur, A. Oliver, T. Sugimoto, M. Matsui, H. Kim, G. Allred, J. Zajicek, Y. Kotani, *Energy Environ. Sci.*, 2012, **5**, 5941.
 - J. Muldoon, C. B. Bucur, A. G. Oliver, J. Zajicek, G. D. Allred, W. C. Boggess, *Energy Environ. Sci.*, 2013, **6**, 482.
 - S. Yagi, A. Tanaka, Y. Ichikawa, T. Ichitsubo, E. J. Matsumura, *Electrochem. Soc.*, 2013, **160**, C83.
 - Y. Chen, T. Liui, Y. Shao, M. H. Engelhard, J. Liu, G. Li, *J. Mater. Chem. A*, 2014, **2**, 2473.
 - E. G. Nelson, J. W. Kampf, B. M. Bartlett, *Chem. Commun.*, 2014, **50**, 5193.
 - F. Wang, Y. Guo, J. Yang, Y. Nuli, S. Hirano, *Chem. Commun.*, 2012, **48**, 10763.
 - H. Gizbar, Y. Vestfrid, O. Chusid, Y. Gofer, H. E. Gottlieb, V. Mrks, D. Aurbach, *Organometallics*, 2004, **23**, 3826.
 - a) Y. Guo, F. Zhang, J. Yang, F. Wang, Y. NuLi, S. Hirano, *Energy Environ. Sci.*, 2012, **5**, 9100. b) Z. Zhao-Karger, X. Zhao, O. Fuhr, M. Fichtner, *RSC Adv.*, 2013, **3**, 16330.
 - O. Mizrahi, N. Amir, E. Pollak, O. Chusid, V. Marks, H. Gottlieb, L. Larush, E. Zinigrad, D. Aurbach, *J. Electrochem. Soc.*, 2008, **155**, A103.
 - N. Pour, Y. Gofer, D. T. Major, D. Aurbach, *J. Am. Chem. Soc.*, 2011, **133**, 6270.
 - B. Liu, T. Luo, G. Mu, X. Wang, D. Chen, G. Shen, *ACS Nano*, 2013, **7**, 8051.
 - R. Kershaw, M. Vlasse, A. Wold, *Inorg. Chem.*, 1967, **6**, 1599.
 - T. Ichitsubo, T. Adachi, S. Yagi, T. Doi, *J. Mater. Chem.*, 2011, **21**, 11764.
 - Z. Huang, T. Mases, Y. Orikasa, T. Mori, T. Minato, C. Tassel, Y. Kobayashi, H. Kageyama, Y. Uchimoto, *J. Mater. Chem. A*, 2014, DOI: 10.1039/C4TA01779J.
 - N. Pour, Y. Gofer, D. T. Major, D. Aurbach, *J. Am. Chem. Soc.*, 2011, **133**, 6270.
 - A. Benmayza, M. Ramanathan, T. S. Arthur, M. Matsui, F. Mizuno, J. Guo, P. Glans, J. Prakash, *J. Phys. Chem. C.*, 2013, **117**, 26881.